JTTEE5 15:663-669
DOI: 10.1361/105996306X147261
1059-9630/$19.00 © ASM International

Effect of Substrate Hardness on Splat Morphology in High-Velocity Thermal Spray Coatings

W. Trompetter, M. Hyland, D. McGrouther, P. Munroe, and A. Markwitz

(Submitted February 23, 2006; in revised form May 4, 2006)

In this study, Ni-chrome alloy particles were thermally sprayed onto a variety of substrate materials using the high-velocity air fuel (HVAF) technique. Although the various substrate materials were sprayed using identical powder material and thermal spray conditions, the type and variation of splat morphologies were strongly dependent on the substrate material. Predominantly solid splats are observed penetrating deeply into softer substrates, such as aluminum, whereas molten splats were observed on harder substrates, which resisted particle penetration. The observed correlation between molten splats and substrate hardness could be due a dependency of deposition efficiencies of solid and molten splats on the substrate material. However, it was found that conversion of particle kinetic energy into plastic deformation and heat, dependent on substrate hardness, can make a significant contribution towards explaining the observed behavior.

Keywords coating-substrate interaction, HVAF, splat temperature, substrate hardness.

1. Introduction

In general, the temperature of the powder material being coated is dependent on the thermal spray technique used. The cold spray process only slightly heats the spray coating material (<300 °C) (Ref 1) and usually produces solid splats. The plasma spray process uses very high temperatures (>3800 °C) (Ref 2), producing only molten droplets. High-velocity oxyfuel (HVOF) and high-velocity air fuel (HVAF) thermal spray methods cover the intermediate temperature region where sprayed particles reach temperatures in the range of 500-2500 °C (Ref 2, 3). For the HVOF/HVAF methods, the solid or molten state of the particle depends on the heat gained during acceleration in a hot gas plus the conversion of the particle kinetic energy into heat, relative to the melting point of the particle material. The microstructure of the resultant splats will ultimately affect the bulk thermal, mechanical, and electrical properties of the coating. The high-velocity spray processes are interesting in this respect because a wide spectrum of splat thermal states will be sprayed. In this paper, the influence of the substrate on resultant splat microstructures for NiCr splats deposited by HVAF thermal spray is examined.

This article was originally published in *Building on 100 Years of Success: Proceedings of the 2006 International Thermal Spray Conference* (Seattle, WA), May 15-18, 2006, B.R. Marple, M.M. Hyland, Y.-Ch. Lau, R.S. Lima, and J. Voyer, Ed., ASM International, Materials Park, OH, 2006.

W. Trompetter, National Isotope Centre, GNS Sciences, Lower Hutt, New Zealand and Department of Chemical and Materials Engineering, University of Auckland, New Zealand; **M. Hyland,** Department of Chemical and Materials Engineering, University of Auckland, Auckland, New Zealand; **D. McGrouther** and **P. Munroe,** Electron Microscope Unit, University of New South Wales, Sydney, Australia; and **A. Markwitz,** National Isotope Centre, GNS Sciences, Lower Hutt, New Zealand. Contact e-mail: btrompetter@gns.cri.nz.

2. Experimental Procedures

Commercial Ni-chrome alloy powder (Ni80/Cr20, 5-45 μm), supplied from Sulzer Metco (Winterthor, Switzerland), was thermally sprayed onto a variety of substrate materials listed in Table 1, using the HVAF thermal spraying technique (Ref 3). The substrates were clamped between 2 mm thick steel plates, for support and as a heat sink during HVAF thermal spraying. This would reduce any possible effects of substrate thickness variations on the results. HVAF is a low-temperature thermal spray process, compared with HVOF, where their typical combustion temperatures have been estimated (Ref 3) to be ~1870 and 2650 °C, respectively. The gas cools as it leaves the combustion chamber and expands into the nozzle where the gas jet achieves supersonic expansion. Hence, the gas temperature in the nozzle, where the feedstock powder is inserted, is much lower than the gas temperature in the combustion chamber. For a chamber pressure of 414 kPa (60 psi), the gas temperature falls to ~1300 °C in the diverging section of the nozzle (Ref 3), which is below the melting point of NiCr powder (T_m = 1400 °C). In addition, the contact time of the spray particles with the gas jet is quite short (~200 μs for a particle velocity of 700 m s^{-1} and a spray distance of 150 mm), and the particles will become only partially heated. As the spray particles and gas travel from the gun to the substrate, the gas continues to cool as it expands, resulting in particles with high kinetic energy but with low thermal energies.

The morphology of the splats was investigated with a focused ion beam (FIB) microscope and cross-sectional scanning electron microscopy (SEM). The FEI xP200 (FEI, Portland, OR) FIB miller (Ref 4, 5) uses a focused beam of 30 keV gallium ions which is scanned over the surface of a specimen. The gallium beam at low currents (10-70 pA) can be used to produce images with resolution <100 nm of the sample via secondary electrons emitted during interactions of the ions with the specimen. Alternatively, at high currents (1000-7000 pA), the beam can be used to rapidly sputter away the specimen to expose a cross-sectioned surface without the distortion or alteration found in other sectioning techniques. A further capability of the FIB is the ability to produce very thin (~100 nm) sections at almost any

Table 1 Substrates deposited with single splat particles

Substrate	Source	Thickness, mm	Purity, %
Al	Alcan NZ 1200	1.2	99.50
Cu	HC high conductivity	3.0	99.90
Fe	Cold-rolled steel	2.0	99.70
Ti	Goodfellow Ti foil	0.25	99.6
Ta	Goodfellow Ta foil	1.0	99.9
C	Goodfellow glassy carbon	1.0	100
Si	MMRC, polished, [1, 0, 0]	0.5	100

desired location in a sample, suitable for examination by transmission electron microscopy (TEM) as well as the ability to section splats for investigating splat-substrate interfaces. FIB images were used to determine splat diameters. The diameter of the splash splats was measured to where the splat started to solidify (i.e., the splash fingers were not included). Splat heights could also be determined from FIB images of sectioned splats.

3. Results

A wide variety of splat formations were observed when Nichrome alloy particles were thermally sprayed onto a variety of substrates with varying hardnesses using the HVAF technique. Although identical conditions were used during thermal spraying, the amount of different types of splats varied significantly for different substrate materials. Images of splat microstructures on the various substrates are shown in Fig. 1 and summarized in Table 2 and Fig. 2. Three types of "splat" morphologies are observed:

- *Solid splats:* During the thermal spray process, the temperature (T) remains below the melting point (T_m) of the spray coating material ($T < T_m$) (Ref 6-8). Images of sectioned solid splats can be seen in Fig. 1(a).
- *Slushy/broken/semimolten:* During the thermal spray process, particles are thermally softened or partial melting of the particle occurs. Additionally, during impact, further localized heating can occur due to conversion of kinetic energy to heat energy from plastic deformation of the particle ($T \approx T_m$) (Ref 9). Images of semimolten splats can be seen in Fig. 1(b).
- *Molten ("splash" splats and "disc" splats):* For particles that become molten during the spray coating process, two types of splats can be observed: "splash" splats and "disc" splats. Splash splats occur when the splat starts to solidify before the splat has come to rest ($T > T_m$). Disc splats occur when the splat solidifies after the splat has come to a rest and has stopped spreading ($T \gg T_m$) (Ref 10). Images of "splash splats" and "disk splats" can be seen in Fig. 1(c) and (d), respectively.

Predominantly solid splats with minimal deformation were observed penetrating deeply into softer substrates such as aluminum. Conversely, splats were observed to deform strongly when incident on harder substrates, such as silicon, which resisted particle penetration. In addition, a higher incidence of molten splats was observed on harder substrates.

Table 2 and Fig. 2 are quantitative overviews of splat types observed on a variety of different substrate materials. Note that the distribution of splat types varied markedly with substrate type. As expected, few solid splats were found on the harder substrates, as such splats probably rebound after impact. For harder substrates, predominantly slushy and molten splats adhered. For soft substrates such as aluminum, NiCr particles penetrated deeply into the substrate material, forming a mixture of solid and broken splats. Interestingly, the softer substrates had proportionally fewer molten splats; on aluminum, only 3% of the splats were molten.

FIB cross sections in Fig. 1(a) show the extent of substrate deformation by solid NiCr particles. Measurements of sectioned NiCr splats showed that they frequently embed into aluminum substrates, displacing a substrate volume comparable to the particle volume. Conversely, sectioned NiCr splats on harder substrates such as glassy carbon or silicon showed that the NiCr splats displaced very little substrate volume comparable to the splat volume.

The relationship between substrate hardness and particle deformation was investigated by measuring splat flattening ratios (Fig. 3) and diameters (Fig. 4, 5). Figure 3 shows that:

- Splats with flattening ratios <1.4 remain solid.
- Splats with flattening ratios between 1.4 and 1.9 become broken, slushy, or melt.

Splats with flattening ratios >1.9 were not sectioned but were found to be molten splats. Dykhuizen (Ref 6) also found that particle flattening depends on substrate hardness and particle temperature.

Figure 5 shows that, in general, the size range of the solid splats observed on the various substrate materials is representative of the powder feedstock (5-45 μm). However, the size range of molten splats (Fig. 4) indicates that, in general, there is a relationship with the substrate hardness. In particular, molten splats on the softer substrates have a smaller size range, whereas the harder substrates have a larger size range. This may be due to a greater collection efficiency of larger molten splats on harder substrates, a greater degree of spreading of the splats on the harder surfaces, or more plastic deformation of solid splats on harder substrates causing more heat and strain energy, which melts previously solid particles.

4. Discussion

The most significant difference in the splat distributions on the substrates studied is the lack of molten splats on the softer substrates and the preponderance of molten splats on the harder substrates. The relationship between the type of splat and substrate hardness shown in the results could be due to several different effects. For example,

- The relationship between deposition efficiencies for solid and molten splats may depend on the substrate material.
- In the process of plastic deformation, some of the particle kinetic energy can be converted into heat and strain energy, which can melt a previously solid particle.

In the literature, modeling the impact of "splats" onto substrates has been described for both solid (Ref 6-8) and molten (Ref 10) splats. For fully molten droplets, the substrate hardness is generally not considered an important influence on the splat formation morphology and is not included in splat flattening formulae found in the literature. Conversely, for solid particles impacting on a substrate, the substrate hardness plays an intimate/important role in the final profile of a splat. Additionally, in cold spray deformation models, melting is not considered because, in general, the particles have not been observed to melt (Ref 6-8). Interfacial melting has been observed only in a few cold spray coatings (Ref 11, 12). In the process of plastic deformation,

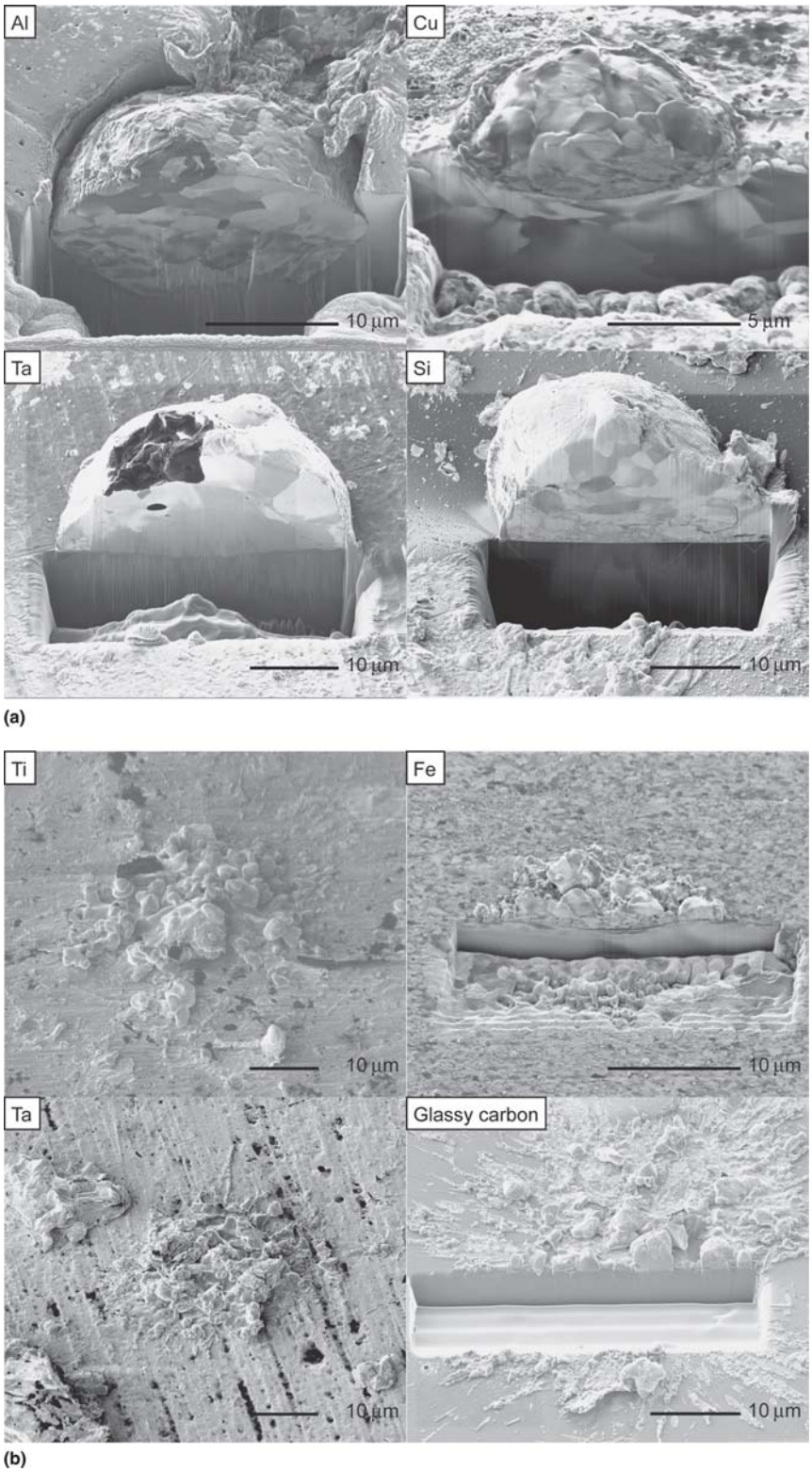

Fig. 1 (a) Solid splats (some sectioned) on various types of substrates HVAF sprayed with NiCr particles; (b) semimolten splats (some sectioned) on various types of substrates HVAF sprayed with NiCr particles; (c) molten-splash splats on various types of substrates HVAF sprayed with NiCr particles; (d) molten-disc splats on various types of substrates HVAF sprayed with NiCr particles

some of the particles' kinetic energy can be converted into heat and strain energy, which can melt a previously solid particle. Hence, there is a gap in the available models covering the region of thermal spray processes where heated solid particles can become molten during the impact process. This has only recently been discussed by Vleck (Ref 11).

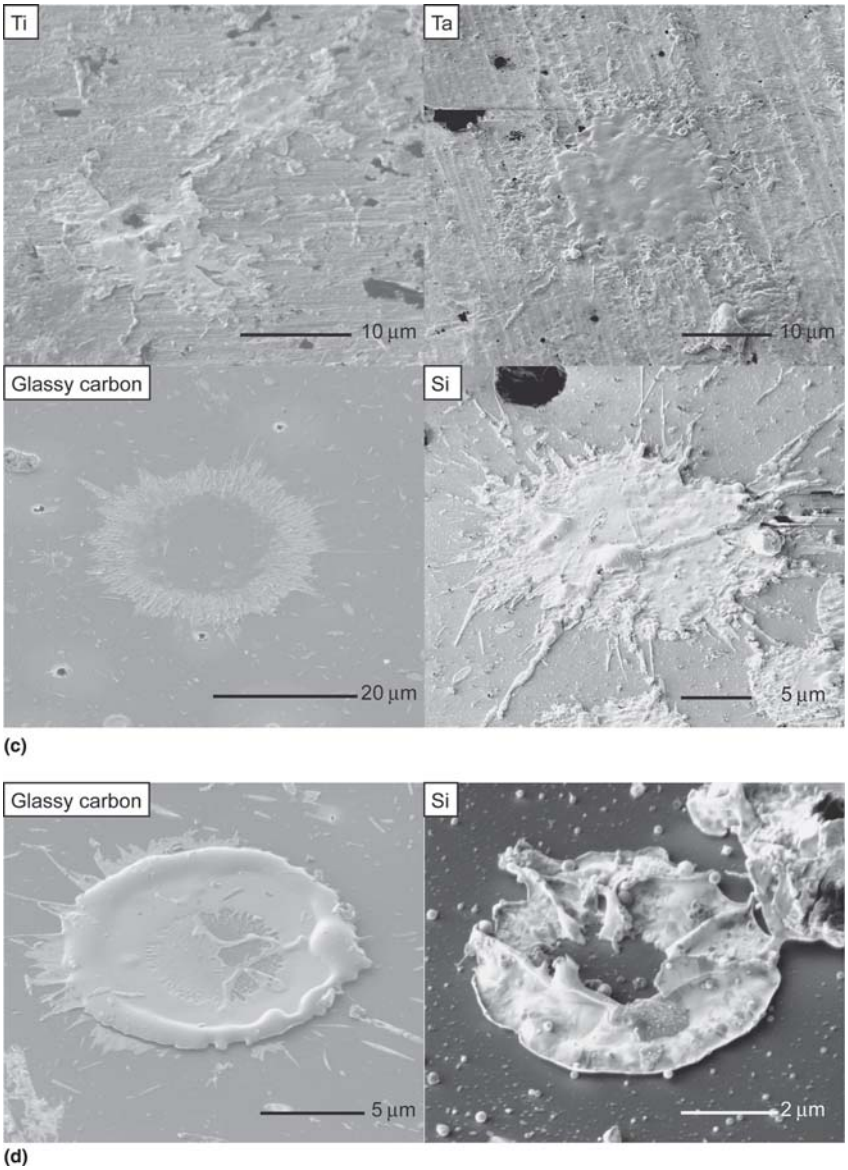

Fig. 1 (cont.) (a) Solid splats (some sectioned) on various types of substrates HVAF sprayed with NiCr particles; (b) semimolten splats (some sectioned) on various types of substrates HVAF sprayed with NiCr particles; (c) molten-splash splats on various types of substrates HVAF sprayed with NiCr particles; (d) molten-disc splats on various types of substrates HVAF sprayed with NiCr particles

To test the feasibility of this notion, an estimate of the particle temperature both before and after impact was made from which the expected fraction of solid and molten splats was determined. The estimate is based on two energy components:

- Heat gained during acceleration from the hot gas in the HVAF gun.
- Conversion of particle kinetic energy into heat during impact.

4.1 Estimation of Heat Gained during Acceleration in the HVAF Gun

The average particle velocity, temperature and their distributions were not measured during the HVAF coating, however typical values can be obtained from the literature. For a chamber pressure of 414 kPa (60 psi), it has been estimated that the average particle velocity is 670 m s^{-1} (2222 ft s^{-1}) and the average gas temperature is ~1274 °C (2326 °F) in the diverging section of the nozzle (Ref 3), which is below the melting point of NiCr powder (T_m = 1400 °C). Hence, the majority of the impacting NiCr splats are expected to be solid. The temperature distribution of particles from the similar HVOF coating process has been measured (Ref 13) and was found to follow a Gaussian distribution with an average value of 2119 °C with a standard deviation of 296 °C (14%). For the purposes of this paper, a similar Gaussian distribution with a 14% standard deviation will be used to approximate the temperature distribution of particles in HVAF thermal coating.

4.2 Estimation of Particle Kinetic Energy Conversion into Heat during Impact

NiCr particles deformed very little when impacted into soft substrates such as aluminum. Hence, very little of the particles'

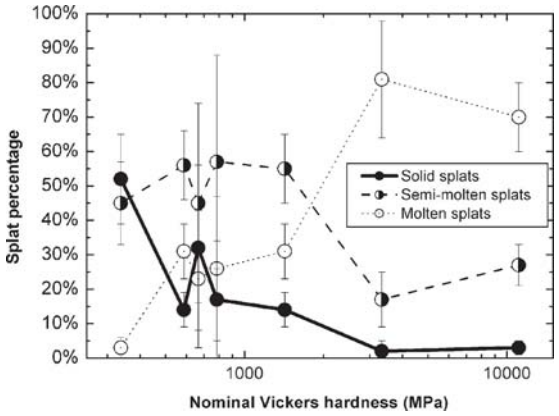

Fig. 2 Graph of splat type percentage vs. substrate hardness (error bars represent 2 SD)

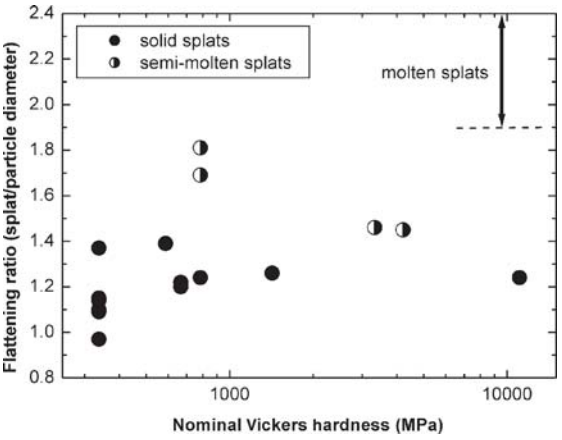

Fig. 3 Plot of splat flattening ratio (splat diameter/pre-impact particle diameter) vs. substrate hardness

Table 2 Survey results of splat morphology types on various substrates

Substrate	Nominal Vickers hardness, MPa	Yield strength, MPa	Solid splats, %	Semi-molten splats, %	Molten splats, %
Al	338	10-35	52	45	3
Ti	588	140-250	14	56	31
Cu	667	54	32	45	23
Fe	785	120-150	17	57	26
Ta	1422	310-380	14	55	31
C	3334	…	2	17	81
Si	11,082	1000-2000	3	27	70

kinetic energies (e.g., 5%) would have been converted into plastic deformation and heat. Conversely, NiCr particles suffered heavy deformation impacting into hard substrates. In this case, most of the particles kinetic energy (e.g., 95%) would have been converted into plastic deformation and heat.

To calculate the particle temperature after impact, a heat capacity (C_p) of 0.460 J K^{-1} g^{-1} and an estimated enthalpy of fusion (ΔH_{fus}) of 286 J g^{-1} were used as outlined in Table 3 and shown in Fig. 6. Heat conduction during the collision process can be ignored and assumed to be adiabatic, i.e., heat transfer does not need to be considered (Ref 1, 6, 7).

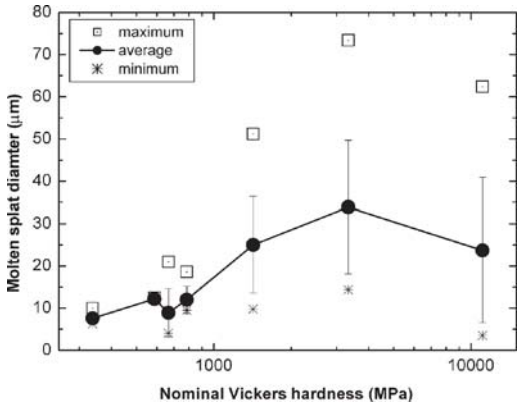

Fig. 4 Molten splat diameter vs. substrate hardness (error bars represent 1 SD)

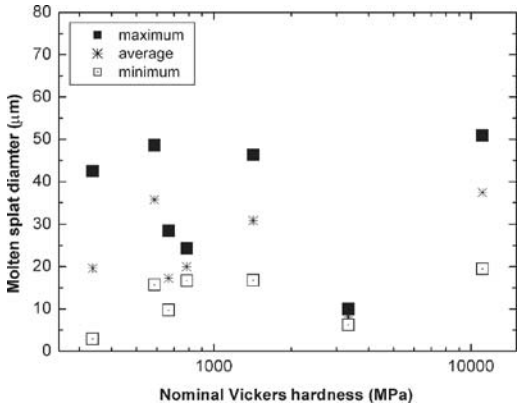

Fig. 5 Solid splat diameter vs. substrate hardness (error bars represent 1 SD)

The pre-impact Gaussian distribution with an average temperature of 1274 °C (2326 °F) and a standard deviation of 14% (178 °C) is estimated to be predominantly solid particles. The effect of additional particle heating from the conversion of the particle kinetic energy into plastic deformation and heat was considered. In Table 4, the splat temperature plus the percentage of solid and molten splats, was estimated for different percentages of kinetic energy transferred into heat energy. In the calculations, an average pre-impact particle temperature (T_p) of 1274 °C with a standard deviation of 14% and an average particle velocity of 670 m s^{-1} was used. It was found that, when 90% of the kinetic energy is transferred into heat energy, only 8% of the splats were estimated to be molten. However, if the average particle velocity is increased by 46% to 975 m s^{-1}, the estimate of molten splats increases to 80%, which is similar to the observed percentage of molten splats on hard substrates. In Table 5, the percentage of solid and molten splats for varying amounts of kinetic energy transferred into heat energy were calculated using an average particle velocity of 975 m s^{-1}. These results show a similar trend with the percentages of solid and molten splats observed on the spray-coated samples for soft and hard substrates in Fig. 1.

Measurements of HVOF particle velocities show distributions with standard deviations similar to the temperature distribution (Ref 14, 15). Previous studies have observed threshold velocity behavior (Ref 7) where thermal spraying is successful

Table 3 Relationship between splat energy and temperature

Splat thermal energy	Temperature region	Splat temperature
$E_{thermal} = T_p \times C_p$	$T_p < T_m$	$T_p = E_{thermal}/C_p$
For $E_{thermal} > T_m \times C_p$ and $T_p \times C_p \Delta H_{fus} < T_m \times C_p$	$T_p = T_m$	$T_p = T_m$
$E_{thermal} = T_p \times C_p + \Delta H_{fus}$	$T_p > T_m$	$T_p = (E_{thermal} - \Delta H_{fus})/C_p$

only above a critical velocity. Particles below the critical velocity have insufficient energy to break surface oxides and achieve sufficient plastic deformation for successful bonding.

Although it has been shown that the substrate (and splat) hardness appears to be the primary cause of the additional heating due to the splat deformation, other material properties of the substrate (and splat) are also likely to influence the splat formation. Theoretical studies of solid particle impacts (Ref 1, 6, 7) have shown that heat conduction during the collision process can be ignored and assumed to be adiabatic. For molten splat impacts, it has been shown (Ref 10) that heat transfer due to the substrate and splat thermal conductivity, particle wetting properties does influence the final morphology of molten splats.

5. Conclusions

NiCr alloy particles were thermally sprayed onto a variety of substrate materials using the HVAF technique. Soft substrates predominantly had deeply penetrating solid splats, whereas harder substrates that resisted particle penetration had a higher percentage of molten splats. Although the observed correlation between molten splats and substrate hardness could be due a dependency of the deposition efficiencies for solid and molten splats on the substrate material, a more promising explanation can originate from the conversion of particle kinetic energy into heat depending on the amount of plastic deformation due to substrate hardness. In the process of plastic deformation, some of the particles kinetic energy can be converted into heat and strain energy, which can melt a previously solid particle. The percentage of kinetic energy transferred into heat energy appears to be greater for harder substrates.

The expected fraction of solid and molten splats on different substrates were estimated based on the heat gained during the particle acceleration in the HVAF gun and the conversion of particle kinetic energy into heat during impact. To achieve estimated percentages of molten splats, similar to the observed percentages of molten splats on soft and hard substrates, it was necessary to use a higher average particle velocity of 975 m s^{-1}. The use of a velocity ~50% higher than the expected is consistent with studies where successful particle bonding is observed only above a critical velocity. Particles below the critical velocity have insufficient energy to break surface oxides and achieve sufficient plastic deformation for successful bonding. Hence, the conversion of particle kinetic energy into heat can make a significant contribution toward explaining the observed correlation between molten splats and substrate hardness.

Acknowledgments

The authors thank Steve Mathews, previously of Auckland University, and Holsters Engineering in Tokoroa for assistance with HVAF thermal spray sample preparation.

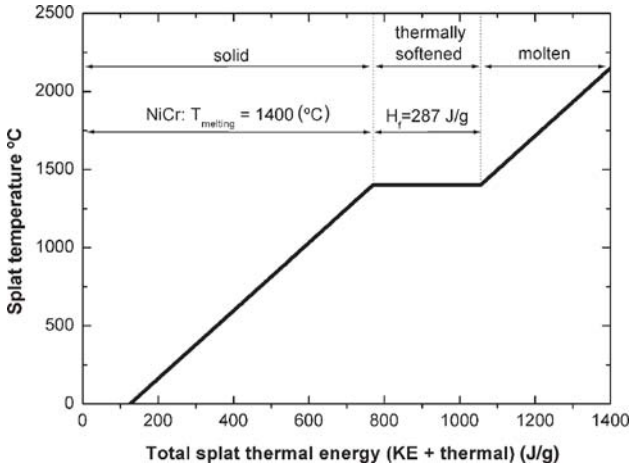

Fig. 6 Relationship between splat thermal energy and temperature

Table 4 Percentages of solid and molten splats for varying amounts of KE transferred into heat energy (T_p = 1274 °C, SD = 14%, particle velocity = 670 m s^{-1})

KE transferred into heat energy, %	Solid, %	Molten, %
0	100	0
5	100	0
10	100	0
25	100	0
50	99	1
75	96	4
90	92	8
100	88	12

Table 5 Percentages of solid and molten splats for varying amounts of KE transferred into heat energy (T_p = 1274 °C, SD = 14%, particle velocity = 975 m s^{-1})

KE transferred into heat energy, %	Solid, %	Molten, %
0	100	0
5	100	0
10	100	0
25	99	1
50	85	15
75	44	56
90	20	80
100	9	91

References

1. H. Assadi, F. Gärtner, T. Stoltenhoff, and H. Kreye, Bonding Mechanism in Cold Gas Spraying, *Acta Mater.,* 2003, **51,** p 4379-4394
2. R.W. Smith, Equipment and Theory, *A Lesson from Thermal Spray Technology,* ASM International, 1992, Course 51, Lesson, Test 2
3. J.A. Browning, Hypervelocity Impact Fusion: A Technical note, *J. Therm. Spray. Technol.,* 1992, **1**(4), p 289-292
4. N. Rowlands and P. Munroe, FIB for the Evaluation of Non-Semiconductor Materials, *Microstruct. Sci.,* 1998, **26,** p 26-29
5. J.M. Cairney, R.D. Smith, and P.R. Munroe, Transmission Electron Microscope Specimen Preparation of Metal Matrix Composites Using the Focused Ion Beam Miller, *Microsc. Microanal.,* 2000, **5,** p 452-462
6. R.C. Dykhuizen, M.F. Smith, D.L. Gilmore, R.A. Neiser, X. Jiang, and S. Sampath, Impact of High Velocity Cold Spray Particles, *J. Therm. Spray. Technol.,* 1999, **8**(4), p 559-564

7. T.H. Van Steenkiste, J.R. Smith, and R.E. Teets, Aluminum Coatings via Kinetic Spray with Relatively Large Powder Particles, *Surf. Coat. Technol.,* 2002, **154**(2-3), p 237-252
8. M. Grujicic, J.R. Saylor, D.E. Beasley, W.S. DeRosset, and D. Helfritch, Computational Analysis of the Interfacial Bonding between Feed-Powder Particles and the Substrate in the Cold-Gas Dynamic-Spray Process, *Appl. Surf. Sci.,* 2003, **219,** p 211-227
9. T.C. Hanson, C.M. Hackett, and G.S. Settles, Independent Control of HVOF Particle Velocity and Temperature, *J. Therm. Spray. Technol.,* 2002, **11**(1), p 75-85
10. P. Fauchais, M. Fukumoto, A. Vardelle, and M. Vardelle, Knowledge Concerning Splat Formation: An Invited Review, *J. Therm. Spray. Technol.,* 2004, **13**(3), p 337-360
11. J. Vleck, L. Gimeno, H. Huber, and E. Lugscheider, A Systematic Approach to Material Eligibility for the Cold Spray Process, *J. Therm. Spray. Technol.,* 2005, **14**(1), p 125-133
12. J. Vleck, H. Huber, H. Voggenreiter, and E. Lugscheider, "Melting upon Particle Impact in the Cold Spray Process," Presented at Materials Week 2002, International Congress on Advanced Materials, Their Processes and Applications, September 30–October 2, 2002 (Munich, Germany), DGM
13. J.R. Fincke, D.C. Haggard, and W.D. Swank, Particle Temperature Measurement in the Thermal Spray Process, *J. Therm. Spray. Technol.,* 2001, **10**(2), p 255-266
14. M. Li, D. Shi, and P.D. Christofides, Diamond Jet Hybrid HVOF Thermal Spray: Gas-Phase and Particle Behavior Modeling and Feedback Control Design, *Ind. Eng. Chem. Res.,* 2004, **43,** p 3632-3652
15. K.A. Kowalsky, D.R. Marantz, M.F. Smith, and W.L. Oberkampf, HVOF: Particle Flame Diagnostics and Coatings Characteristics, *Proc. 3rd Nat. Conf. Therm. Spray,* T.F Bernecki, Ed., May 20–25, 1990 (Long Beach, CA), ASM International, 1991, p 587-596